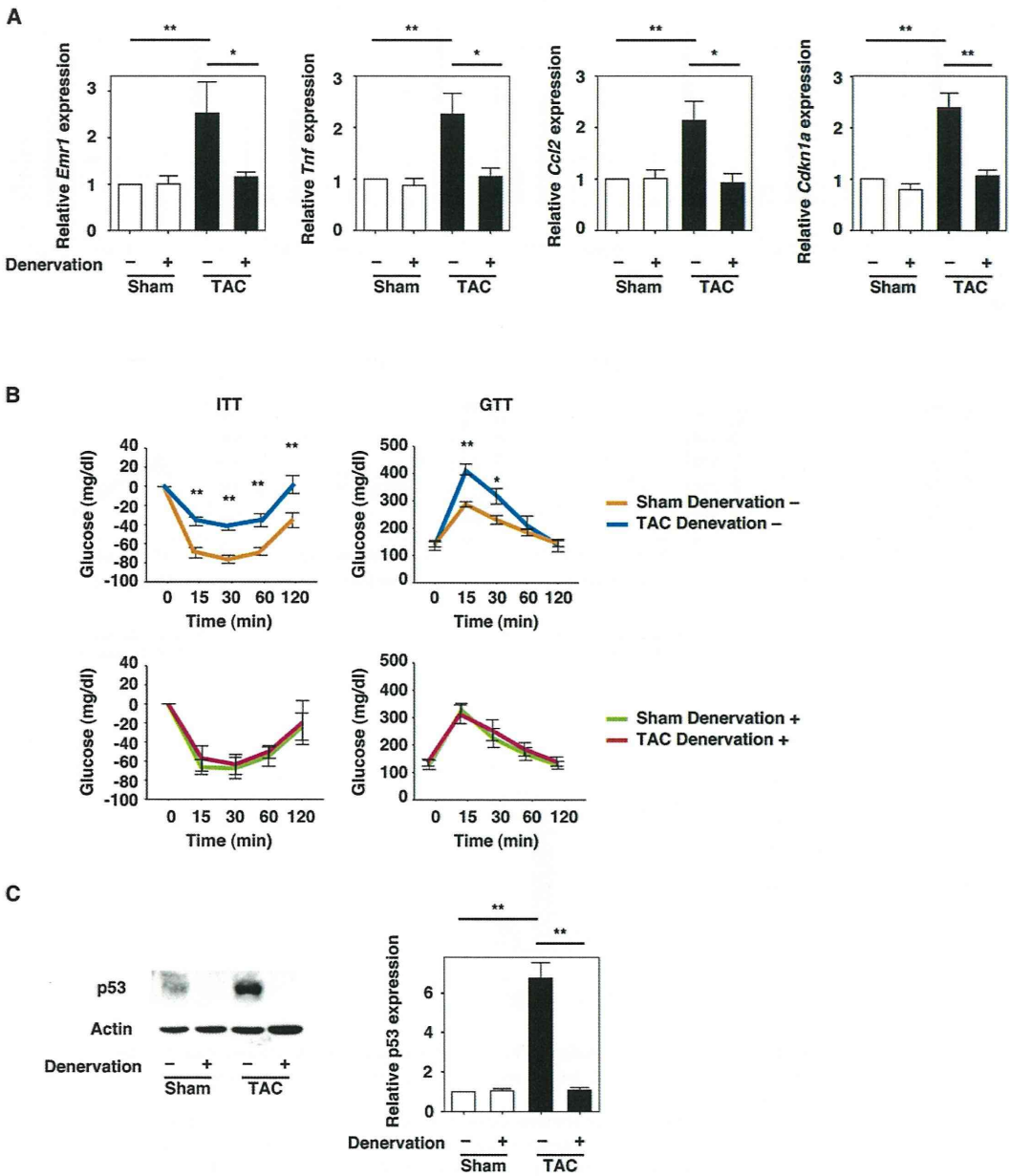

Figure 3. Surgical Transection of the Sympathetic Nerves Attenuates Adipose Tissue Inflammation and Systemic Insulin Resistance

(A) Real-time PCR assessing the expression of *Emr1*, *Tnf* (Tnfα), *Ccl2* (MCP1), and *Cdkn1a* (p21) levels in adipose tissues of mice at 6 weeks after sham operation (Sham) or TAC with or without surgical transection of the sympathetic nerves (Denervation) of epididymal fat (n = 8).

(B) Insulin tolerance test (ITT) and glucose tolerance test (GTT) of mice at 6 weeks after sham operation (Sham) or TAC with or without surgical denervation (n = 20).

(C) Western blot analysis of p53 in adipose tissues of mice at 6 weeks after sham operation (Sham) or TAC with or without surgical denervation. The right graph indicates the quantitative data on p53 expression (n = 3). Data are shown as the means ± S.E.M. *p < 0.05, **p < 0.01.

tissue p53 expression and inflammation (Figures S5H–S5J). Inhibition of p53 activation in adipose tissue by genetic disruption significantly attenuated inflammation of this tissue and improved metabolic abnormalities (Figures S5K and S5L). These results suggest that the same mechanism underlies insulin resistance associated with heart failure due to both pressure overload and MI.

Influence of Inhibiting p53-Induced Adipose Tissue Inflammation on Cardiac Function

To investigate whether inhibition of p53-induced adipose tissue inflammation could influence cardiac function in the development of heart failure, we performed TAC and monitored cardiac function in adipo-p53 KO mice. We found that adipo-p53 KO mice showed significantly better cardiac function and less LV

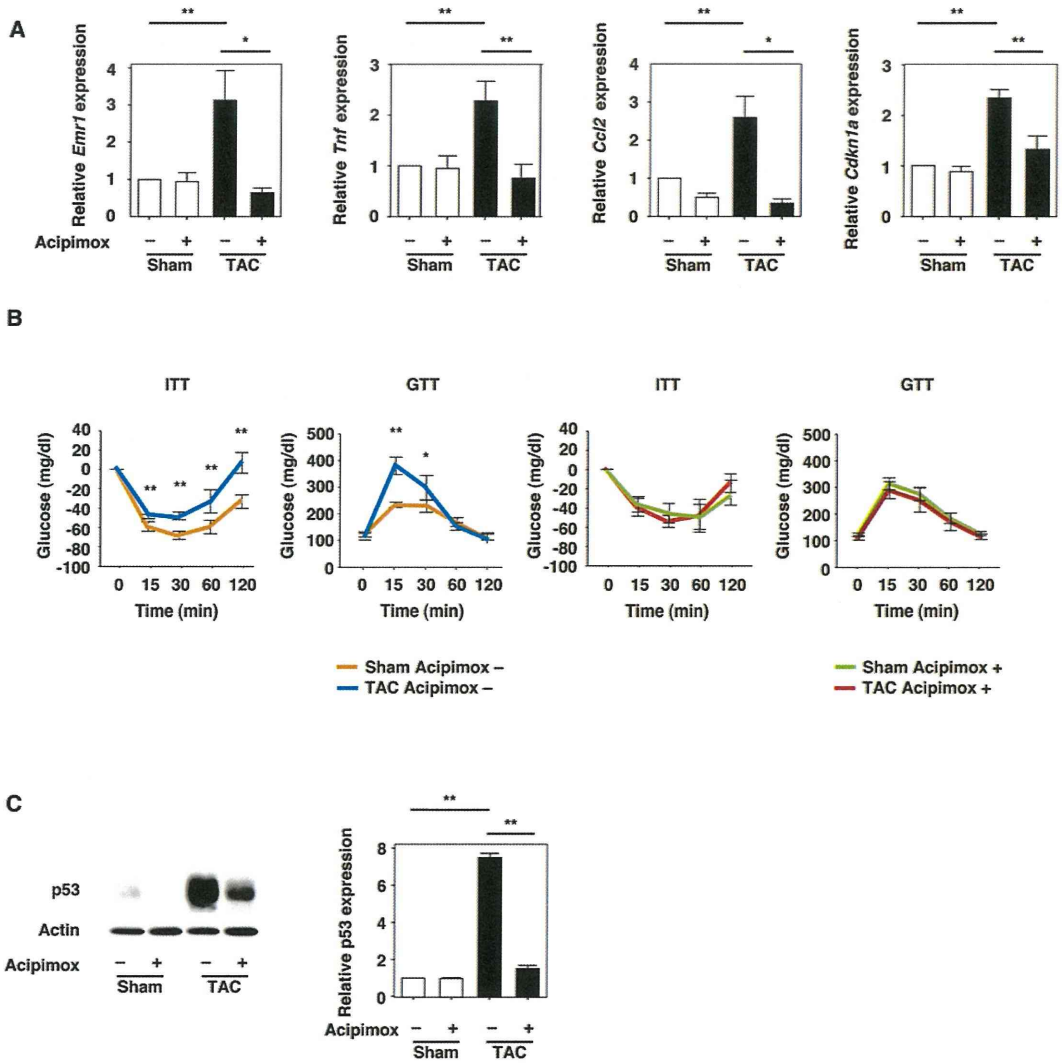

Figure 4. Treatment with a Lipolysis Inhibitor Ameliorates Adipose Tissue Inflammation and Systemic Insulin Resistance

(A) Real-time PCR assessing the expression of *Emr1*, *Tnf* (Tnfα), *Ccl2* (MCP1), and *Cdkn1a* (p21) levels in adipose tissue of mice at 6 weeks after sham operation (Sham) or TAC with or without acipimox treatment (n = 8).

(B) Insulin tolerance test (ITT) and glucose tolerance test (GTT) of mice at 6 weeks after sham operation (Sham) or TAC with or without acipimox treatment (n = 32).

(C) Western blot analysis of p53 in adipose tissues of mice at 6 weeks after sham operation (Sham) or TAC with or without acipimox treatment. Actin was used as an equal loading control. The right graph indicates the quantitative data on p53 expression (n = 3). Data are shown as the means ± S.E.M. *p < 0.05, **p < 0.01.

enlargement compared with their littermate controls (Figure 6A). They also showed better survival during the chronic phase of heart failure (Figure 6B). Similar results were observed in another model of heart failure induced by MI (Figure S6A). Furthermore, administration of a p53 inhibitor (pifithrin-α) into the adipose tissue of the TAC or MI model mice after the onset of heart failure improved cardiac dysfunction, as well as adipose tissue inflammation, and metabolic abnormalities (Figures 6C–6E and S6B–S6D), indicating that inhibition of p53 may be useful for the treatment of heart failure and its associated metabolic abnormalities. Moreover, we noted significant improvement of cardiac function after sympathetic nerve blockade (Figures S6E and S6F). However, treatment of TAC mice with acipimox was found to exacerbate cardiac dysfunction (Figure S6G), presumably because it impaired fatty acid metabolism and energy production in cardiomyocytes, as reported previously (Tuunanen et al., 2006).

Mechanism of p53-Induced Adipose Tissue Inflammation during Heart Failure

Because our results indicated that adrenergic activation induced lipolysis that upregulated p53 and promoted adipose tissue inflammation, we speculated that an excess of fatty acids might be involved in the upregulation of p53 in adipose tissue. Therefore, we examined the effect of palmitic acid on cultured preadipocytes. Treatment with palmitic acid significantly increased the

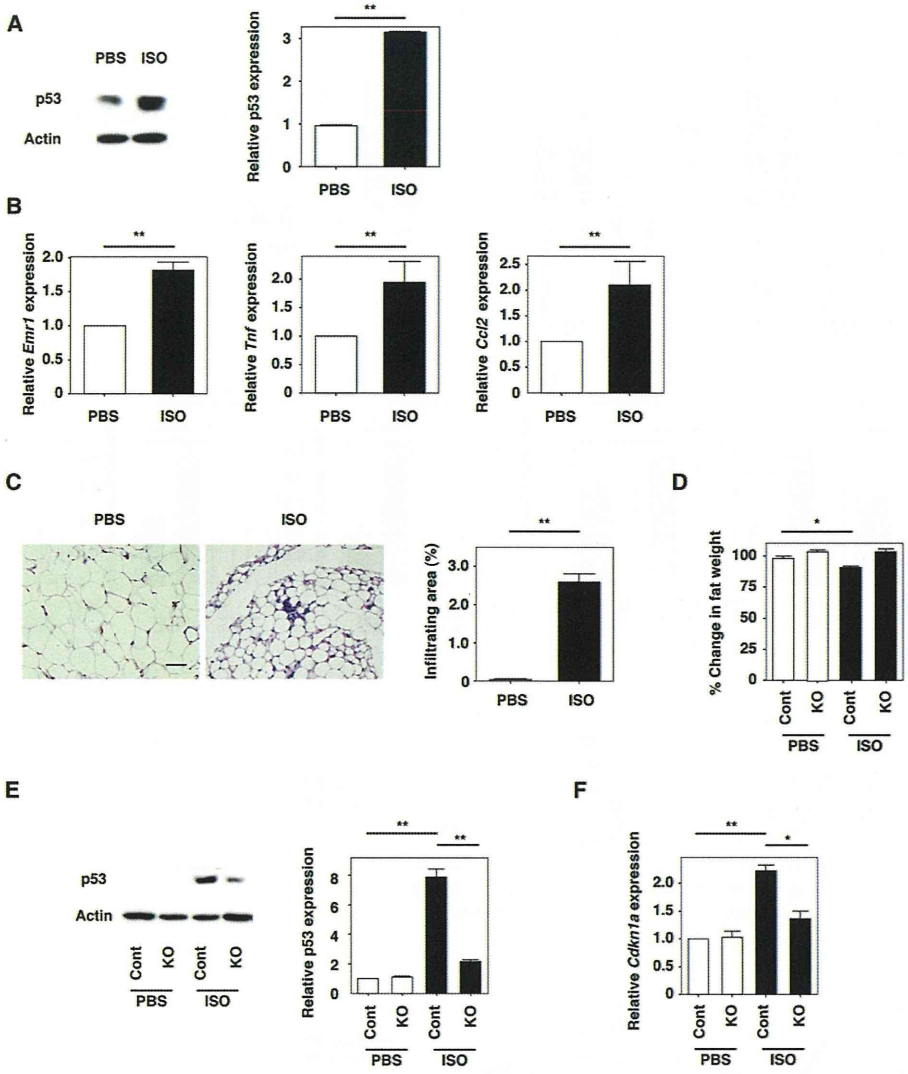

Figure 5. Role of Lipolysis in the Regulation of Adipose p53 Expression and Inflammation

(A) Western blot analysis of p53 in adipose tissues of wild-type mice treated with PBS or isoproterenol (ISO). Actin was used as an equal loading control. The right graph indicates the quantitative data on p53 expression (n = 3).

(B) Real-time PCR assessing the expression of *Emr1*, *Tnf* (Tnfα), and *Ccl2* (MCP1) levels in adipose tissues of wild-type mice treated with PBS or isoproterenol (ISO) (n = 8).

(C) Hematoxylin and eosin staining of adipose tissues of wild-type mice treated with PBS or isoproterenol (ISO). Scale bar, 50 μm. The right graph indicates the quantitative data on macrophage infiltration (n = 4).

(D) The changes in weight of adipose tissues isolated from Atgl-deficient mice (KO) and littermate controls (Cont) after treatment with PBS or isoproterenol (ISO) (n = 6).

(E) Expression of p53 was examined in adipose tissues of Atgl-deficient mice (KO) and littermate controls (Cont) treated with PBS or isoproterenol (ISO) by western blot analysis. The right graph indicates the quantitative data on p53 expression (n = 3).

(F) Real-time PCR assessing the expression of *Cdkn1a* (p21) level in adipose tissues isolated from Atgl-deficient mice (KO) and littermate controls (Cont) after treatment with PBS or isoproterenol (ISO) (n = 6). Data are shown as the means ± S.E.M. *$p < 0.05$, **$p < 0.01$.

intracellular level of reactive oxygen species (ROS) and caused DNA damage, as demonstrated by the increase of γH2AX, which in turn upregulated p53 expression (Figures 7A–7C, S7A, and S7B). This upregulation of p53 was associated with an increase of NF-κB activity and proinflammatory cytokine expression (Figures 7D and 7E). Because it has been reported that p53 enhances the activity of NF-κB, which regulates various cytokines including *TNF-α* and *CCL2* (Benoit et al., 2006; Ryan et al., 2000), we examined the relationship between p53 expression and NF-κB activation. We demonstrated that the disruption of p53 expression significantly attenuated palmitic acid-induced activation of NF-κB and upregulation of *Ccl2*

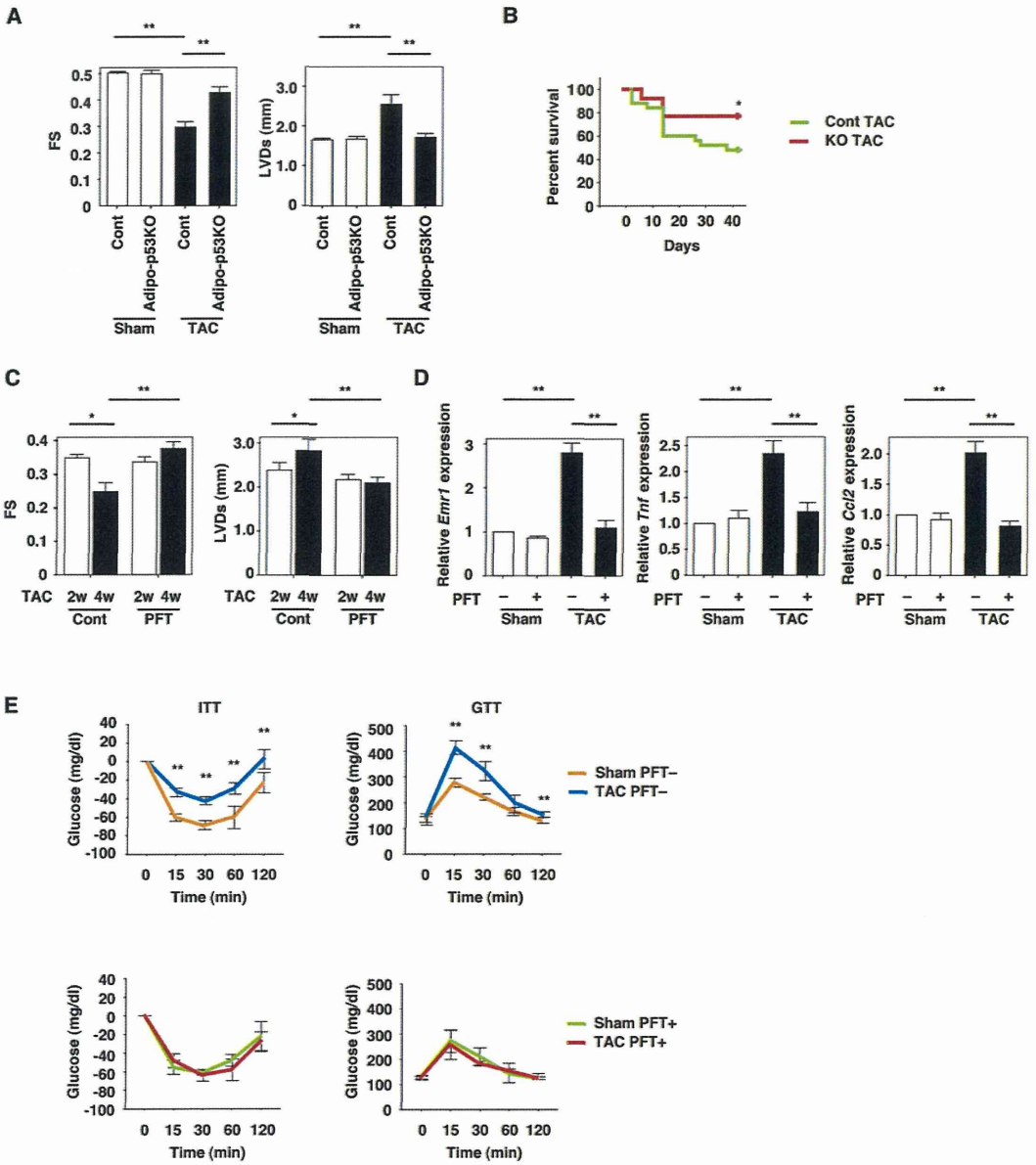

Figure 6. Influence of Inhibiting p53-Induced Adipose Tissue Inflammation on Cardiac Function

(A) Echocardiography to assess systolic function (FS) and ventricular size (LVDs) in adipocyte-specific p53-deficient mice (adipo-p53 KO) and littermate controls (Cont) at 6 weeks after sham operation or TAC (n = 8). FS, fractional shortening; LVDs, left ventricular end-systolic diameter.

(B) Survival rate of adipocyte-specific p53-deficient mice (adipo-p53 KO) and littermate controls (Cont) after TAC procedure (n = 25).

(C) Pifithrin-α (PFT) was administered into the adipose tissue of mice at 2–4 weeks after TAC, and systolic function (FS) and ventricular size (LVDs) were estimated before (2w, 2 weeks after TAC) and after (4w, 4 weeks after TAC) treatment by echocardiography (n = 5).

(D) Real-time PCR assessing the expression of *Emr1*, *Tnf* (Tnfα), and *Ccl2* (MCP1) levels in adipose tissue of mice at 4 weeks after sham operation or TAC with or without pifithrin-α (PFT) treatment (n = 4).

(E) Insulin tolerance test (ITT) and glucose tolerance test (GTT) of mice at 4 weeks after sham operation or TAC with or without pifithrin-α (PFT) treatment (n = 12).

Data are shown as the means ± S.E.M. *p < 0.05, **p < 0.01.

(Figures 7D and 7E), whereas knockdown of the NF-κB component p50 markedly inhibited palmitic acid-induced upregulation of *Ccl2* (Figure 7E). In addition, treatment with an antioxidant inhibited palmitic acid-induced DNA damage and upregulation of p53 (Figures S7A and S7B). We also found that ROS and γH2AX expression were increased in the adipose tissue of mice with heart failure (Figures 7F and 7G). Furthermore, nuclear localization of p50 was enhanced in adipose tissue during heart failure (Figures 7H and S7C). This increase of nuclear p50 expression and the upregulation of proinflammatory cytokines

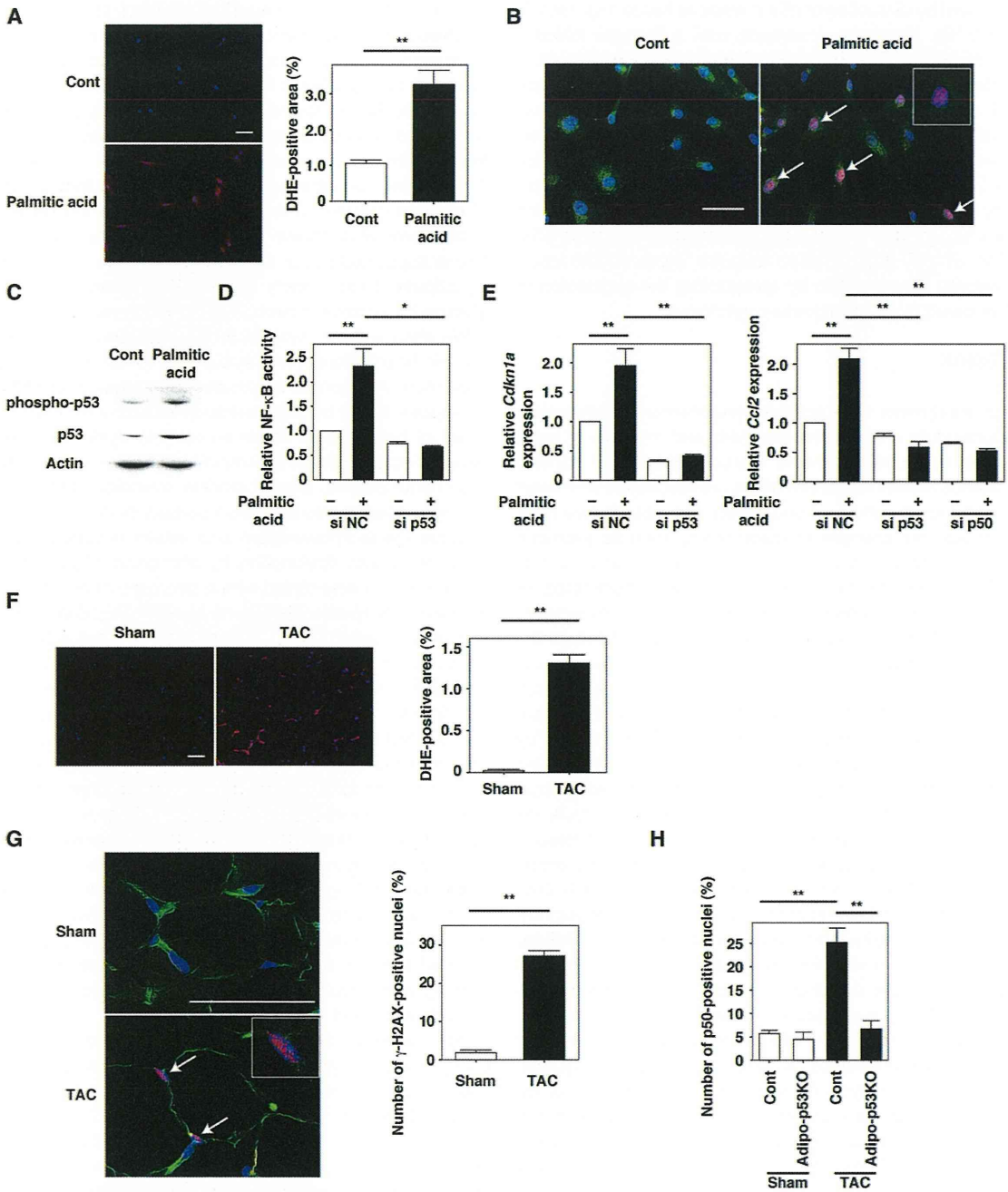

Figure 7. Mechanism of p53-Induced Adipose Tissue Inflammation during Heart Failure

(A) Dihydroethidium (DHE) staining (red) of preadipocytes treated with vehicle (Cont) or palmitic acid (500 μM) for 10 min. Nuclei were stained with Hoechst dye (blue). Scale bar indicates 50 μm. The right graph indicates the quantitative data on DHE-positive area (n = 4).

(B) Immunofluorescent staining for γ-H2AX (red) in preadipocytes treated with vehicle (Cont) or palmitic acid (500 μM) for 1 hr. Nuclei and plasma membranes were stained with Hoechst dye (blue) and Wheat Germ agglutinin lectin (green). Scale bar indicates 50 μm.

(C) Western blot analysis of phospho-p53 and p53 expression in preadipocytes treated with vehicle (Cont) or palmitic acid (500 μM).

(D) Small-interfering RNA targeting p53 (sip53) or negative control RNA (siNC) was introduced into preadipocytes treated with or without palmitic acid (500 μM) for 12 hr. The NF-κB activity was examined by luciferase assay (n = 5).

(E) Real-time PCR assessing the expression of *Cdkn1a* (p21) and *Ccl2* (MCP1) levels in preadipocytes prepared in Figure 7D (n = 9). The effect of small-interfering RNA targeting the NF-κB component p50 (sip50) on the expression of *Ccl2* (MCP1) was also examined (n = 9).

(F) Dihydroethidium (DHE) staining (red) in adipose tissue from sham-operated (Sham) and TAC mice. Nuclei were stained with Hoechst dye (blue). Scale bar indicates 20 μm. The right graph indicates the quantitative data on DHE-positive area (n = 5).

were inhibited by disruption of p53 in adipose tissue (Figures 2B, 7H, and S7C). Moreover, treatment with a lipolysis inhibitor significantly inhibited the heart failure-induced increase of ROS and nuclear p50 expression (Figures S7D and S7E). Inhibition of NF-κB activation in adipose tissue by BAY 11-7082 also significantly attenuated adipose tissue inflammation and improved metabolic abnormalities and cardiac dysfunction in TAC mice (Figures S7F–S7H). These results indicate that adrenergic activation by heart failure induces lipolysis in adipose tissue, which increases DNA damage due to ROS and thus upregulates p53. Activation of p53 then induces adipose tissue inflammation and metabolic abnormalities by upregulating the expression of NF-κB-dependent proinflammatory cytokines.

DISCUSSION

Although treatments that achieve neurohumoral antagonism have successfully reduced the morbidity and mortality of heart failure, the death rate remains unacceptably high (Kannel, 2000). Various metabolic abnormalities are associated with heart failure, and recent data have suggested that heart failure itself promotes adverse changes of metabolism, such as systemic insulin resistance (Ashrafian et al., 2007; Witteles and Fowler, 2008). Thus, a detrimental vicious cycle may be postulated, in which heart failure induces insulin resistance that in turn accelerates cardiac dysfunction (Opie, 2004). However, studies on the molecular mechanisms of such metabolic abnormalities in heart failure are largely preliminary and the results have sometimes been conflicting. In the present study, we demonstrated a causal role for heart failure in the development of insulin resistance by using two mouse models of heart failure, and we elucidated the underlying mechanisms. We found that the hyperadrenergic state of heart failure initiated a vicious metabolic cycle by promoting lipolysis in adipose tissue that increased the release of free fatty acids and upregulated p53 expression and proinflammatory cytokine production in adipose tissue, which then promoted systemic insulin resistance. Cardiac insulin resistance is considered to contribute to the development of heart failure. Because excessive cardiac insulin signaling has been reported to exacerbate systolic dysfunction in both TAC and MI models (Shimizu et al., 2010), hyperinsulinemia associated with systemic insulin resistance may also have a pathological role in heart failure until insulin resistance becomes evident in the myocardium. Inhibition of lipolysis by sympathetic denervation or by treatment with a lipolysis inhibitor improved insulin resistance in our heart failure model. Plasma free fatty acid levels were significantly elevated after the onset of heart failure, whereas this increase was attenuated by inhibition of lipolysis with acipimox, denervation, or guanethidine. Disruption of p53 in adipose tissue also markedly attenuated adipose inflammation and metabolic abnormalities associated with heart failure, whereas fatty acid levels were unaffected. Thus, adipose tissue inflammation rather than the increase of plasma free fatty acids per se is involved in the impairment of insulin sensitivity and glucose tolerance associated with heart failure. We also noted that p53 was modestly upregulated in the liver and skeletal muscle, presumably due to the increase of circulating free fatty acids. However, we did not detect a strong inflammatory response in those tissues under our experimental conditions (I. Shimizu and T. Minamino, unpublished data), suggesting that upregulation of adipose tissue p53 is more important for the development of metabolic abnormalities during heart failure. This concept is further supported by our finding that disruption of p53 activation in adipose tissue nearly normalized insulin resistance and glucose intolerance provoked by heart failure.

We observed that systolic cardiac function and survival with chronic heart failure were significantly better for adipo-p53 KO mice than their control littermates. Suppression of p53 activity in adipose tissue by administration of a p53 inhibitor after the onset of heart failure improved cardiac dysfunction and also reduced adipose tissue inflammation and metabolic abnormalities in both the TAC and MI models. Inhibition of NF-κB activity in adipose tissue also improved cardiac dysfunction, as well as adipose tissue inflammation and insulin resistance. Improvement of cardiac dysfunction by disruption of p53 in adipose tissue was not associated with a decrease of plasma free fatty acid levels. Systemic inhibition of lipolysis (Atgl deficiency or acipimox treatment) and disturbance of lipolysis in adipose tissue (denervation or guanethidine treatment) significantly reduced plasma free fatty acid levels (Haemmerle et al., 2006). However, the former intervention accelerated heart failure, whereas cardiac dysfunction was improved by the latter. Thus, the beneficial effect of inhibiting p53-induced adipose tissue inflammation on cardiac function is independent of changes in circulating free fatty acid levels, and lipolysis in cardiomyocytes appears to have a crucial role in cardiac metabolism and energy production. Although there is evidence suggesting that p53 has a protective role against damage due to ROS and lipotoxicity (Bazuine et al., 2009), our results indicate that chronic activation of p53 in adipose tissue causes inflammation and that inhibition of p53-induced adipose tissue inflammation is a potential target for treating metabolic abnormalities and systolic dysfunction in patients with heart failure.

Adipose tissue was traditionally considered to be a simple energy storage organ, but it is now appreciated that it also has endocrine functions and secretes a variety of factors referred to as adipokines (Donath and Shoelson, 2011; Hotamisligil, 2006; Ouchi et al., 2011). With high calorie intake, the size and number of adipocytes increase, and hypertrophic adipocytes shift the balance toward production of proinflammatory adipokines. This shift in the adipokine profile causes the modification of adipose tissue macrophages from the anti-inflammatory M2 type to the proinflammatory M1 type, and further increases the production of proinflammatory molecules, which in turn

(G) The number of γ-H2AX-positive nuclei (white arrows and inset) in adipose tissue of mice at 6 weeks after sham operation (Sham) or TAC procedure was estimated by immunofluorescent staining for γ-H2AX (red) (n = 5). Nuclei and plasma membranes were stained with Hoechst dye (blue) and Wheat Germ agglutinin lectin (green). Scale bar indicates 50 μm.

(H) The number of p50-positive nuclei in adipose tissue of adipocyte-specific p53-deficient mice (adipo-p53 KO) and littermate controls (Cont) at 6 weeks after sham operation (Sham) or TAC procedure was estimated by immunofluorescent staining for p50 (n = 6). Data are shown as the means ± S.E.M. *$p < 0.05$, **$p < 0.01$.

accelerates the recruitment of activated macrophages into inflamed fatty tissue. Adipokines produced by inflamed adipose tissue have been suggested to play a crucial role in the regulation of glucose and lipid metabolism and to contribute to the development of diabetes (Donath and Shoelson, 2011; Hotamisligil, 2006; Ouchi et al., 2011). It has been reported that excessive calorie intake leads to accumulation of ROS in adipose tissue and subsequently causes DNA damage that activates p53 (Minamino et al., 2009). In contrast to obesity, heart failure decreases body fat tissue mass by inducing lipolysis. Accelerated lipolysis and a subsequent increase of free fatty acids are likely to cause p53 activation because we found that the promotion of lipolysis by treatment with isoproterenol upregulated adipose tissue expression of p53, whereas inhibition of lipolysis by acipimox or disruption of lipase activity attenuated p53 expression. These results are consistent with a recent report describing that fasting-induced lipolysis promotes an immune response in murine adipose tissue (Kosteli et al., 2010). Various molecular mechanisms of p53 activation by heart failure may be postulated, including hypoxia, increased oxidative stress, and induction of endoplasmic reticulum stress (Harris and Levine, 2005; Schenk et al., 2008). Our in vitro and in vivo studies have indicated that an increase of free fatty acids causes ROS-induced DNA damage that upregulates p53 in adipose tissue. Activation of p53 then upregulates the expression of proinflammatory adipokines via the NF-κB signaling pathway and promotes systemic insulin resistance.

The β-blockers are competitive antagonists of β-adrenergic receptors. At one time, β-blockers were contraindicated in patients with heart failure due to their negative inotropic effect. However, several large-scale clinical trials demonstrated the efficacy of β-blockers for reducing morbidity and mortality in heart failure patients with impaired systolic function, so β-blockers are now recommended as first-line agent for these patients (Hjalmarson et al., 2000; Leizorovicz et al., 2002; Packer et al., 2001, 2002). A reduction of heart rate due to inhibition of cardiac β_1-adrenergic receptors is believed to be responsible for most of the therapeutic benefits associated with β-blocker treatment, although this is not the only mechanism of action that may be important in heart failure. It is interesting that treatment with a nonselective β-blocker (carvedilol) achieved a more marked improvement of survival in patients with chronic heart failure than treatment with a β_1-selective blocker (metoprolol) (Poole-Wilson et al., 2003), whereas new-onset diabetes was frequent in heart failure patients during treatment with the β_1-selective blocker (Torp-Pedersen et al., 2007). It has been reported that carvedilol antagonizes the β_3-adrenergic receptor as well as the $\beta_{1/2}$-adrenergic receptors (Schnabel et al., 2000). Taking our results together with these reports, it seems that inhibition of β_3-adrenergic activity in adipose tissue partially accounts for the better clinical outcome in patients treated with this nonselective β-blocker. Recent evidence has suggested that treatment with insulin sensitizers improves systolic function of the failing heart in animal models (Asakawa et al., 2002; Nemoto et al., 2005) but such treatment increases the incidence of heart failure in diabetic patients, presumably because of sodium retention (Home et al., 2009). Inhibition of p53-induced adipose tissue inflammation could be an alternative therapeutic target to block the metabolic vicious cycle in patients with heart failure.

EXPERIMENTAL PROCEDURES

Animal Models

All animal study protocols were approved by the Chiba University review board. C57BL/6 mice were purchased from the SLC Japan (Shizuoka, Japan). TAC and MI were performed in 11-week-old male mice as described previously (Harada et al., 2005; Sano et al., 2007). Sham-operated mice underwent the same procedure except for aortic constriction. Mice that expressed Cre recombinase in adipocytes (Fabp4-Cre) were purchased from Jackson Laboratories. We then crossed Fabp4-Cre mice (with a C57BL/6 background) with mice that carried floxed *Trp53* alleles with a C57BL/6 background (Marino et al., 2000) to generate adipocyte-specific p53 knockout mice. The genotype of littermate controls was Fabp4-Cre$^-$ *Trp53* $^{flox/flox}$. The generation and genotyping of Atgl-deficient mice has been described previously (Haemmerle et al., 2006). Surgical or chemical denervation was performed before TAC operation as described previously (Demas and Bartness, 2001; Foster and Bartness, 2006), with slight modification. In brief, the epididymal fat pad was gently separated from the skin and the abdominal wall by using a dissecting microscope. For surgical denervation, a drop of 1% toluidine blue was applied to the fat pad to facilitate visualization of the nerves. The nerves were then freed from the surrounding tissue and vasculature and cut in two or more locations, and the segments were removed to prevent possible reconnection. Chemical denervation was performed by the local injection of guanethidine sulfate (400 μg, Santa Cruz) into bilateral epididymal fat. Sham-operated mice for surgical denervation underwent the same procedure except for transection of the nerve. For the control group for chemical denervation, saline was injected into adipose tissue rather than guanethidine. Acipimox (Sigma) were provided in drinking water (at a concentration of 0.05%) for 6 weeks after TAC operation as described previously (Guo et al., 2009). Isoproterenol (30 mg/kg/day, Sigma) were delivered by infusion pump (DURECT Corporation) for 2 weeks as described previously (Iaccarino et al., 1999). The local injection of pifithrin-α (2.2 mg/kg/week, Carbiochem) or BAY 11-7082 (20 mg/kg/week, Carbiochem) into bilateral epididymal fat was performed to inhibit adipose p53 or NF-κB activity, respectively, from 2 weeks to 4 weeks after operation.

Physiological and Histological Analyses

Echocardiography was performed with a Vevo 770 High Resolution Imaging System (Visual Sonics Inc, Toronto, Ontario, Canada). To minimize variation of the data, the heart rate was always approximately 550–650 beats per minute when cardiac function was assessed. Epididymal fat samples were harvested and fixed in 10% formalin overnight. The samples were embedded in paraffin and sectioned (Narabyouri research Co., Ltd). The sections were subjected to immunohistochemistry or HE staining. The antibodies used are Mac3-specific primary antibody (PharMingen) for macrophages, p50-specific primary antibody (Cell signaling), and phospho-H2AX-specific antibody (Cell signaling).

Laboratory Tests

For the intraperitoneal glucose tolerance test (IGTT), mice were starved for 6 hr and were given glucose intraperitoneally at a dose of 2 g / kg (body weight) in the early afternoon. For the insulin tolerance test, mice were given human insulin intraperitoneally (1 U / kg body weight) at 1:00 pm without starvation. Blood glucose levels were measured with a glucose analyzer (Roche Diagnostics). We analyzed free fatty acid (Biovision, Inc) and norepinephrine levels (LDN) by using ELISA-based immunoassay kits according to the manufacturer's instruction.

Western Blot Analysis

The lysates were resolved by SDS-polyacrylamide gel electrophoresis. Proteins were transferred to a polyvinylidene difluoride membrane (Millipore, Bedford, MA), which was incubated with the primary antibody followed by anti-rabbit or anti-mouse immunoglobulin-G conjugated with horseradish peroxidase (Jackson, West Grove, PA).

Cell Culture

Human preadipocytes were purchased from Sanko (Tokyo, Japan) and were cultured according to the manufacturer's instructions. NIH 3T3-L1 cells were cultured in high-glucose DMEM plus 10% fetal bovine serum.

Ex Vivo Culture

Epididymal fat was extracted from Atgl-deficient or littermate mice at 17 weeks of age. Freshly isolated fat pads (100–120 mg) were incubated in Dulbecco's modified Eagle's medium supplemented with 10% fetal bovine serum in the presence of isoproterenol (10 μM) for 48 hr. Fat pads were treated with PBS instead of isoproterenol in the control group.

Statistical Analysis

Data are shown as the mean ± SEM. Differences between groups were examined by Student's t-test or ANOVA followed by Bonferroni's correction for comparison of means. For survival analysis, the Kaplan-Meier method and log-rank test were used. For all analyses, $p < 0.05$ was considered statistically significant.

SUPPLEMENTAL INFORMATION

Supplemental Information includes Supplemental Experimental Procedures and seven figures and can be found with this article online at doi:10.1016/j.cmet.2011.12.006.

ACKNOWLEDGMENTS

We thank A. Berns (The Netherlands Cancer Institute) for floxed p53 mice, T. Fujita (The Tokyo Metropolitan Institute of Medical Science) for reagents, and E .Takahashi, M. Iijima, and I. Sakamoto for their excellent technical assistance. This work was supported by a Grant-in-Aid for Scientific Research from the Ministry of Education, Culture, Sports, Science and Technology of Japan and grants from the Ono Medical Research Foundation; the Uehara Memorial Foundation; the Daiichi-Sankyo Foundation of Life Science; the NOVARTIS Foundation for the Promotion Science; the Japan Diabetes Foundation; the Mitsui Life Social Welfare Foundation; the Naito Foundation; the Japanese Society of Anti-Aging Medicine; and the Mitsubishi Pharma Research Foundation (to T.M.); a Grant-in-Aid for Scientific Research from the Ministry of Education, Science, Sports, and Culture and Health and Labor Sciences Research Grants (to I.K.); and a Grant-in-Aid for Scientific Research from the Ministry of Education, Science, Sports, and Culture, and Health and a grant from the Uehara Memorial Foundation, Takeda Science Foundation, and Kowa Life Science Foundation (to I.S.).

Received: June 10, 2011
Revised: October 27, 2011
Accepted: December 9, 2011
Published online: January 3, 2012

REFERENCES

Arnlöv, J., Lind, L., Zethelius, B., Andrén, B., Hales, C.N., Vessby, B., and Lithell, H. (2001). Several factors associated with the insulin resistance syndrome are predictors of left ventricular systolic dysfunction in a male population after 20 years of follow-up. Am. Heart J. *142*, 720–724.

Asakawa, M., Takano, H., Nagai, T., Uozumi, H., Hasegawa, H., Kubota, N., Saito, T., Masuda, Y., Kadowaki, T., and Komuro, I. (2002). Peroxisome proliferator-activated receptor gamma plays a critical role in inhibition of cardiac hypertrophy in vitro and in vivo. Circulation *105*, 1240–1246.

Ashrafian, H., Frenneaux, M.P., and Opie, L.H. (2007). Metabolic mechanisms in heart failure. Circulation *116*, 434–448.

Bazuine, M., Stenkula, K.G., Cam, M., Arroyo, M., and Cushman, S.W. (2009). Guardian of corpulence: a hypothesis on p53 signaling in the fat cell. Clin. Lipidol. *4*, 231–243.

Benoit, V., de Moraes, E., Dar, N.A., Taranchon, E., Bours, V., Hautefeuille, A., Tanière, P., Chariot, A., Scoazec, J.Y., de Moura Gallo, C.V., et al. (2006). Transcriptional activation of cyclooxygenase-2 by tumor suppressor p53 requires nuclear factor-kappaB. Oncogene *25*, 5708–5718.

Demas, G.E., and Bartness, T.J. (2001). Novel method for localized, functional sympathetic nervous system denervation of peripheral tissue using guanethidine. J. Neurosci. Methods *112*, 21–28.

Donath, M.Y., and Shoelson, S.E. (2011). Type 2 diabetes as an inflammatory disease. Nat. Rev. Immunol. *11*, 98–107.

Edwards, M.G., Anderson, R.M., Yuan, M., Kendziorski, C.M., Weindruch, R., and Prolla, T.A. (2007). Gene expression profiling of aging reveals activation of a p53-mediated transcriptional program. BMC Genomics *8*, 80.

Floras, J.S. (2009). Sympathetic nervous system activation in human heart failure: clinical implications of an updated model. J. Am. Coll. Cardiol. *54*, 375–385.

Foster, M.T., and Bartness, T.J. (2006). Sympathetic but not sensory denervation stimulates white adipocyte proliferation. Am. J. Physiol. Regul. Integr. Comp. Physiol. *291*, R1630–R1637.

Guo, W., Wong, S., Pudney, J., Jasuja, R., Hua, N., Jiang, L., Miller, A., Hruz, P.W., Hamilton, J.A., and Bhasin, S. (2009). Acipimox, an inhibitor of lipolysis, attenuates atherogenesis in LDLR-null mice treated with HIV protease inhibitor ritonavir. Arterioscler. Thromb. Vasc. Biol. *29*, 2028–2032.

Haemmerle, G., Lass, A., Zimmermann, R., Gorkiewicz, G., Meyer, C., Rozman, J., Heldmaier, G., Maier, R., Theussl, C., Eder, S., et al. (2006). Defective lipolysis and altered energy metabolism in mice lacking adipose triglyceride lipase. Science *312*, 734–737.

Harada, M., Qin, Y., Takano, H., Minamino, T., Zou, Y., Toko, H., Ohtsuka, M., Matsuura, K., Sano, M., Nishi, J., et al. (2005). G-CSF prevents cardiac remodeling after myocardial infarction by activating the Jak-Stat pathway in cardiomyocytes. Nat. Med. *11*, 305–311.

Harris, S.L., and Levine, A.J. (2005). The p53 pathway: positive and negative feedback loops. Oncogene *24*, 2899–2908.

Hjalmarson, A., Goldstein, S., Fagerberg, B., Wedel, H., Waagstein, F., Kjekshus, J., Wikstrand, J., El Allaf, D., Vítovec, J., Aldershvile, J., et al; MERIT-HF Study Group. (2000). Effects of controlled-release metoprolol on total mortality, hospitalizations, and well-being in patients with heart failure: the Metoprolol CR/XL Randomized Intervention Trial in congestive heart failure (MERIT-HF). JAMA *283*, 1295–1302.

Home, P.D., Pocock, S.J., Beck-Nielsen, H., Curtis, P.S., Gomis, R., Hanefeld, M., Jones, N.P., Komajda, M., and McMurray, J.J.; RECORD Study Team. (2009). Rosiglitazone evaluated for cardiovascular outcomes in oral agent combination therapy for type 2 diabetes (RECORD): a multicentre, randomised, open-label trial. Lancet *373*, 2125–2135.

Hotamisligil, G.S. (2006). Inflammation and metabolic disorders. Nature *444*, 860–867.

Hotamisligil, G.S., Shargill, N.S., and Spiegelman, B.M. (1993). Adipose expression of tumor necrosis factor-alpha: direct role in obesity-linked insulin resistance. Science *259*, 87–91.

Iaccarino, G., Dolber, P.C., Lefkowitz, R.J., and Koch, W.J. (1999). Bbeta-adrenergic receptor kinase-1 levels in catecholamine-induced myocardial hypertrophy: regulation by beta- but not alpha1-adrenergic stimulation. Hypertension *33*, 396–401.

Ingelsson, E., Sundström, J., Arnlöv, J., Zethelius, B., and Lind, L. (2005). Insulin resistance and risk of congestive heart failure. JAMA *294*, 334–341.

Kamei, N., Tobe, K., Suzuki, R., Ohsugi, M., Watanabe, T., Kubota, N., Ohtsuka-Kowatari, N., Kumagai, K., Sakamoto, K., Kobayashi, M., et al. (2006). Overexpression of monocyte chemoattractant protein-1 in adipose tissues causes macrophage recruitment and insulin resistance. J. Biol. Chem. *281*, 26602–26614.

Kannel, W.B. (2000). Incidence and epidemiology of heart failure. Heart Fail. Rev. *5*, 167–173.

Kosteli, A., Sugaru, E., Haemmerle, G., Martin, J.F., Lei, J., Zechner, R., and Ferrante, A.W., Jr. (2010). Weight loss and lipolysis promote a dynamic immune response in murine adipose tissue. J. Clin. Invest. *120*, 3466–3479.

Leizorovicz, A., Lechat, P., Cucherat, M., and Bugnard, F. (2002). Bisoprolol for the treatment of chronic heart failure: a meta-analysis on individual data of two placebo-controlled studies—CIBIS and CIBIS II. Cardiac Insufficiency Bisoprolol Study. Am. Heart J. *143*, 301–307.

Lopaschuk, G.D., Folmes, C.D., and Stanley, W.C. (2007). Cardiac energy metabolism in obesity. Circ. Res. *101*, 335–347.

Maier, B., Gluba, W., Bernier, B., Turner, T., Mohammad, K., Guise, T., Sutherland, A., Thorner, M., and Scrable, H. (2004). Modulation of mammalian life span by the short isoform of p53. Genes Dev. *18*, 306–319.

Marino, S., Vooijs, M., van Der Gulden, H., Jonkers, J., and Berns, A. (2000). Induction of medulloblastomas in p53-null mutant mice by somatic inactivation of Rb in the external granular layer cells of the cerebellum. Genes Dev. *14*, 994–1004.

Meek, D.W. (2009). Tumour suppression by p53: a role for the DNA damage response? Nat. Rev. Cancer *9*, 714–723.

Minamino, T., and Komuro, I. (2007). Vascular cell senescence: contribution to atherosclerosis. Circ. Res. *100*, 15–26.

Minamino, T., and Komuro, I. (2008). Vascular aging: insights from studies on cellular senescence, stem cell aging, and progeroid syndromes. Nat. Clin. Pract. Cardiovasc. Med. *5*, 637–648.

Minamino, T., Orimo, M., Shimizu, I., Kunieda, T., Yokoyama, M., Ito, T., Nojima, A., Nabetani, A., Oike, Y., Matsubara, H., et al. (2009). A crucial role for adipose tissue p53 in the regulation of insulin resistance. Nat. Med. *15*, 1082–1087.

Nemoto, S., Razeghi, P., Ishiyama, M., De Freitas, G., Taegtmeyer, H., and Carabello, B.A. (2005). PPAR-gamma agonist rosiglitazone ameliorates ventricular dysfunction in experimental chronic mitral regurgitation. Am. J. Physiol. Heart Circ. Physiol. *288*, H77–H82.

Neubauer, S. (2007). The failing heart—an engine out of fuel. N. Engl. J. Med. *356*, 1140–1151.

Nikolaidis, L.A., Sturzu, A., Stolarski, C., Elahi, D., Shen, Y.T., and Shannon, R.P. (2004). The development of myocardial insulin resistance in conscious dogs with advanced dilated cardiomyopathy. Cardiovasc. Res. *61*, 297–306.

Opie, L.H. (2004). The metabolic vicious cycle in heart failure. Lancet *364*, 1733–1734.

Ouchi, N., Parker, J.L., Lugus, J.J., and Walsh, K. (2011). Adipokines in inflammation and metabolic disease. Nat. Rev. Immunol. *11*, 85–97.

Packer, M., Coats, A.J., Fowler, M.B., Katus, H.A., Krum, H., Mohacsi, P., Rouleau, J.L., Tendera, M., Castaigne, A., Roecker, E.B., et al; Carvedilol Prospective Randomized Cumulative Survival Study Group. (2001). Effect of carvedilol on survival in severe chronic heart failure. N. Engl. J. Med. *344*, 1651–1658.

Packer, M., Fowler, M.B., Roecker, E.B., Coats, A.J., Katus, H.A., Krum, H., Mohacsi, P., Rouleau, J.L., Tendera, M., Staiger, C., et al; Carvedilol Prospective Randomized Cumulative Survival (COPERNICUS) Study Group. (2002). Effect of carvedilol on the morbidity of patients with severe chronic heart failure: results of the carvedilol prospective randomized cumulative survival (COPERNICUS) study. Circulation *106*, 2194–2199.

Poole-Wilson, P.A., Swedberg, K., Cleland, J.G., Di Lenarda, A., Hanrath, P., Komajda, M., Lubsen, J., Lutiger, B., Metra, M., Remme, W.J., et al; Carvedilol Or Metoprolol European Trial Investigators. (2003). Comparison of carvedilol and metoprolol on clinical outcomes in patients with chronic heart failure in the Carvedilol Or Metoprolol European Trial (COMET): randomised controlled trial. Lancet *362*, 7–13.

Royds, J.A., and Iacopetta, B. (2006). p53 and disease: when the guardian angel fails. Cell Death Differ. *13*, 1017–1026.

Ryan, K.M., Ernst, M.K., Rice, N.R., and Vousden, K.H. (2000). Role of NF-kappaB in p53-mediated programmed cell death. Nature *404*, 892–897.

Sano, M., Minamino, T., Toko, H., Miyauchi, H., Orimo, M., Qin, Y., Akazawa, H., Tateno, K., Kayama, Y., Harada, M., et al. (2007). p53-induced inhibition of Hif-1 causes cardiac dysfunction during pressure overload. Nature *446*, 444–448.

Schenk, S., Saberi, M., and Olefsky, J.M. (2008). Insulin sensitivity: modulation by nutrients and inflammation. J. Clin. Invest. *118*, 2992–3002.

Schnabel, P., Maack, C., Mies, F., Tyroller, S., Scheer, A., and Böhm, M. (2000). Binding properties of beta-blockers at recombinant beta1-, beta2-, and beta3-adrenoceptors. J. Cardiovasc. Pharmacol. *36*, 466–471.

Sharma, N., Okere, I.C., Duda, M.K., Chess, D.J., O'Shea, K.M., and Stanley, W.C. (2007). Potential impact of carbohydrate and fat intake on pathological left ventricular hypertrophy. Cardiovasc. Res. *73*, 257–268.

Shimizu, I., Minamino, T., Toko, H., Okada, S., Ikeda, H., Yasuda, N., Tateno, K., Moriya, J., Yokoyama, M., Nojima, A., et al. (2010). Excessive cardiac insulin signaling exacerbates systolic dysfunction induced by pressure overload in rodents. J. Clin. Invest. *120*, 1506–1514.

Suskin, N., McKelvie, R.S., Burns, R.J., Latini, R., Pericak, D., Probstfield, J., Rouleau, J.L., Sigouin, C., Solymoss, C.B., Tsuyuki, R., et al. (2000). Glucose and insulin abnormalities relate to functional capacity in patients with congestive heart failure. Eur. Heart J. *21*, 1368–1375.

Tenenbaum, A., Motro, M., Fisman, E.Z., Leor, J., Freimark, D., Boyko, V., Mandelzweig, L., Adler, Y., Sherer, Y., and Behar, S. (2003). Functional class in patients with heart failure is associated with the development of diabetes. Am. J. Med. *114*, 271–275.

Torp-Pedersen, C., Metra, M., Charlesworth, A., Spark, P., Lukas, M.A., Poole-Wilson, P.A., Swedberg, K., Cleland, J.G., Di Lenarda, A., Remme, W.J., and Scherhag, A.; COMET investigators. (2007). Effects of metoprolol and carvedilol on pre-existing and new onset diabetes in patients with chronic heart failure: data from the Carvedilol Or Metoprolol European Trial (COMET). Heart *93*, 968–973.

Tuunanen, H., Engblom, E., Naum, A., Någren, K., Hesse, B., Airaksinen, K.E., Nuutila, P., Iozzo, P., Ukkonen, H., Opie, L.H., and Knuuti, J. (2006). Free fatty acid depletion acutely decreases cardiac work and efficiency in cardiomyopathic heart failure. Circulation *114*, 2130–2137.

Tyner, S.D., Venkatachalam, S., Choi, J., Jones, S., Ghebranious, N., Igelmann, H., Lu, X., Soron, G., Cooper, B., Brayton, C., et al. (2002). p53 mutant mice that display early ageing-associated phenotypes. Nature *415*, 45–53.

Vousden, K.H., and Lane, D.P. (2007). p53 in health and disease. Nat. Rev. Mol. Cell Biol. *8*, 275–283.

Vousden, K.H., and Prives, C. (2009). Blinded by the Light: The Growing Complexity of p53. Cell *137*, 413–431.

Vousden, K.H., and Ryan, K.M. (2009). p53 and metabolism. Nat. Rev. Cancer *9*, 691–700.

Weisberg, S.P., McCann, D., Desai, M., Rosenbaum, M., Leibel, R.L., and Ferrante, A.W., Jr. (2003). Obesity is associated with macrophage accumulation in adipose tissue. J. Clin. Invest. *112*, 1796–1808.

Witteles, R.M., and Fowler, M.B. (2008). Insulin-resistant cardiomyopathy clinical evidence, mechanisms, and treatment options. J. Am. Coll. Cardiol. *51*, 93–102.

Young, M.E., McNulty, P., and Taegtmeyer, H. (2002). Adaptation and maladaptation of the heart in diabetes: Part II: potential mechanisms. Circulation *105*, 1861–1870.

Zeng, L., Wu, G.Z., Goh, K.J., Lee, Y.M., Ng, C.C., You, A.B., Wang, J., Jia, D., Hao, A., Yu, Q., and Li, B. (2008). Saturated fatty acids modulate cell response to DNA damage: implication for their role in tumorigenesis. PLoS ONE *3*, e2329.

Biochemical and Biophysical Research Communications 432 (2013) 519–525

Contents lists available at SciVerse ScienceDirect

Biochemical and Biophysical Research Communications

journal homepage: www.elsevier.com/locate/ybbrc

Ablation of *Rnf213* retards progression of diabetes in the Akita mouse

Hatasu Kobayashi[a,1], Satoru Yamazaki[b,1], Seiji Takashima[c], Wanyang Liu[a], Hiroko Okuda[a], Junxia Yan[a], Yukiko Fujii[a], Toshiaki Hitomi[a], Kouji H Harada[a], Toshiyuki Habu[d], Akio Koizumi[a,*]

[a] Department of Health and Environmental Sciences, Graduate School of Medicine, Kyoto University, Kyoto, Japan
[b] Department of Cell Biology, National Cerebral and Cardiovascular Center, Suita, Osaka, Japan
[c] Department of Molecular Cardiology, Osaka University, Suita, Osaka, Japan
[d] Radiation Biology Center, Kyoto University, Kyoto, Japan

ARTICLE INFO

Article history:
Received 23 January 2013
Available online 11 February 2013

Keywords:
Rnf213
Moyamoya disease
Diabetes
Knockout mouse
Akita mouse

ABSTRACT

Moyamoya disease (MMD) and moyamoya syndrome are vasculopathies characterized by progressive stenosis in the circle of Willis and its branches. The *RNF213* gene, which encodes a novel class of proteins, characterized by both E3 ligase and AAA + ATPase activities, has been identified as the susceptibility gene for MMD. However, its physiological functions remain unknown. MMD and moyamoya syndrome are often accompanied by diabetes mellitus. In this study, we generated *Rnf213* knockout (KO) C57BL/6 mice (*Rnf213*$^{-/-}$; *Ins2*$^{+/+}$), which were mated with Akita (C57BL/6 *Rnf213*$^{+/+}$; *Ins2*$^{+/C96Y}$) mice, a strain that develops diabetes spontaneously by 5 weeks of age, to obtain mice lacking *Rnf213* and carrying the Akita mutation (KO/Akita, *Rnf213*$^{-/-}$; *Ins2*$^{+/C96Y}$). Body weight and blood glucose concentration were measured from 6 to 20 weeks. Glucose tolerance, insulin resistance, plasma insulin and leptin concentrations, food consumption, pancreatic insulin content and histopathology were evaluated at 18 weeks of age. We found that glucose tolerance, as indicated by AUC, was 20% lower ($p < 0.05$) and insulin contents in pancreas were 150% higher ($p < 0.05$), in KO/Akita than in Akita mice. The number of CHOP positive β-cells assayed by histopathological examination was 30% lower and food consumption was 34% lower in KO/Akita than in Akita mice ($p < 0.05$ each). These findings indicated that the disruption of *Rnf213* improved glucose tolerance by protecting islet β cells.

1. Introduction

Moyamoya disease (MMD) and moyamoya syndrome are vasculopathies characterized by occlusion at the internal carotid arteries in the circle of Willis and the compensatory formation of an abnormal vascular network, resembling "puffs of smoke", that are called moyamoya vessels [1]. Patients with moyamoya syndrome have a predisposing disease [2], including Down's syndrome [3], neurofibromatosis 1 [4], or microcephalic osteodysplastic primordial dwarfism type Majewski II (MOPDII) [5], whereas patients with MMD have no such predisposing conditions.

Conditions predisposing to moyamoya syndrome are frequently accompanied by diabetes [2,5–7]. Moreover, the prevalence of type 1 diabetes mellitus was shown to be much higher in patients with MMD than in the general population [8], suggesting a pathological link between MMD and diabetes. We recently demonstrated that *RNF213* was the susceptibility gene for MMD, and that the p.R4810K polymorphism (ss179362673: G>A) is a founder variant commonly found in East Asian patients [9]. Although knockdown of *RNF213* in zebrafish caused abnormal vascular development [9], the physiological function of *RNF213* remains largely unknown.

RNF213 encodes a unique, 591-kDa protein with both a ring finger domain and Walker motifs, and *RNF213* mRNA is expressed in various tissues [9]. The E3 ligase activity of the ring finger domain was confirmed by self-ubiquitination, and ATPase in the Walker motifs was confirmed biochemically [9]. Ring-base E3 ligases have been linked to the control of many cellular processes, including proteasome-dependent proteolysis, DNA repair, signal transduction, apoptosis, immunological processes and transcription [10]. *RNF213* is also an AAA + ATPase because it has Walker A and Walker B motifs. AAA + ATPases usually exist and function as oligomers; their cellular functions include vesicular transport, quality control, cargo trafficking and microtubule homeostasis [11].

In this study, we tested whether ablation of *Rnf213* can modify diabetes mellitus in Akita mice (C57BL/6 *Rnf213*$^{+/+}$; *Ins2*$^{+/C96Y}$), a model for type 1 diabetes [12], in which β-cell destruction results from endoplasmic reticulum (ER) stress. We found that ablation of *Rnf213* unexpectedly alleviates diabetes by preserving β-cell function through moderating the vicious cycle of hyperphagia and hypoinsulinemia.

* Corresponding author. Address: Department of Health and Environmental Sciences, Graduate School of Medicine, Kyoto University, Konoe-cho, Yoshida, Sakyo-ku, Kyoto 606-8501, Japan. Fax: +81 75 753 4458.
E-mail address: koizumi.akio.5v@kyoto-u.ac.jp (A. Koizumi).
[1] These authors contributed equally to this work.

0006-291X/$ - see front matter © 2013 Elsevier Inc. All rights reserved.
http://dx.doi.org/10.1016/j.bbrc.2013.02.015